Bistable tori and long transient dynamics in three coupled identical ring oscillators

Nataliya Stankevich
lab. of Topology methods in dynamics
National Research University
High School of Economics
Nizhny Novgorod, Russia
e-mail stankevichnv@mail.ru

Alexey Kazakov
lab. Dynamical systems and Applications
National Research University
High School of Economics
Nizhny Novgorod, Russia
e-mail kazakovdz@yandex.ru

Evgeny Volkov
dept. of Theoretical Physics
Lebedev Physical Institute
Moscow, Russia
email volkov@td.lpi.ru

***Abstract*—On the example of three coupled identical ring oscillators, the coexistence of two stable homogeneous tori embedded in each other, corresponding to the regimes of successive activity of oscillators, is established. It is shown that a small stable torus is born from a stable periodic regime as a result of supercritical Neirmark-Sacker bifurcation. A large torus is formed as a result of saddle-node bifurcation. We present a study of the formation of tori coexistence as well as long transient dynamics on the threshold of bistability.**

Keywords— quasiperiodic oscillations, multistability, ring oscillators, gene regulatory networks

I. INTRODUCTION

Bistability is one of fundamental properties of nonlinear dynamical systems [1]. The simplest case of multistability can be associated with the bifurcation leading to the loss of symmetry of an equilibrium state, when two equilibrium states symmetrical to each other coexist after the bifurcation. This type of bifurcation corresponds to the so-called Turing bifurcation, which underlies morphogenesis. Another example of the emergence of multistability is associated with generalized Andronov-Hopf bifurcation (it can be Bautin bifurcation, or subcritical Andronov-Hopf bifurcation) when up to the threshold of the bifurcation of the equilibrium state in the phase space, a couple of cycles are generated as a result of the saddle-node bifurcation, one of which is stable and coexists with stable equilibrium. The literature is widely known for many other, more complex examples of bi- and multistability, as well as methods for controlling coexisting equilibria.

The bistability of main dynamical regimes plays a special role in biology. For example, in a recent paper [2], it is suggested that the saddle-node “ghost” can be a minimal dynamical mechanism which enables processing of time-varying growth factor signals. Critical organization in the vicinity of a saddle-node bifurcation enables transient memory of the receptor activity to be realized via the metastable “ghost” state.

The simplest type of multistability, such as the coexistence of equilibrium states, allows us to describe cell proliferation, which in the presence of cell–cell communication, could provide a mechanism for reliable decision making in the presence of noise, by triggering cellular transitions [3]. Multistability can also be implemented for more complex dynamical behavior. For example, the multistability of chaotic attractors with other simpler attractors, or even with other types of chaotic attractors [4] are known. In the framework of this paper, we study a rarer form of multistability, when tori coexist in a phase space of a system.

Quasiperiodic oscillations usually occur in ensembles of non-identical oscillators with the introduction of detuning. Another known mechanism leading to quasiperiodic oscillations in ensembles of identical oscillators is the introducing of coupling through a common mean field [5-7]. Among systems demonstrating such phenomenon, we would like to mention models of synthetic genetic networks (Repressilator), the coupling for which is realized through a common signaling molecule, which forms the mean field [8]. The simplest single Repressilator can be described as a ring of unidirectionally coupled three nonlinear genetic elements. In a recent paper [9], the evolution of a torus in a system of three coupled Repressilators was investigated. In the framework of this work, we will present new aspects of this model related to multistability.

We show the possibility of coexistence between two different tori, describe the mechanism of occurrence of such bistability, and also show examples of the emergence of long transient dynamics at the threshold of occurrence of bistable tori. The model under consideration describes the minimal population of the Repressilators, the connection between which is organized through a sense of density, the so-called quorum-sensing, and we restrict ourselves to small coupling strength.

II. OBJECT OF INVESTIGATION

A. Mathematicla model

We use the model of three three-dimensional ring oscillators with quorum-sensing coupling. Such model represent reduced version of the model for three Repressilators coupled via the production of special signal molecules called “autoinducer”. Fig.1 shows the principle scheme of a single repressilator. Here **a**, **b**, **c** are mRNAs, A, B, C are expressed protein repressors. S is autoinducer (AI) molecule which diffuses through the cell membrane. The resulting equations for the protein concentrations and the concentration S are

$$\begin{aligned}
\dot{A}_i &= \beta_1(-A_i + \frac{\alpha}{1+C_i^n}),\\
\dot{B}_i &= \beta_2(-B_i + \frac{\alpha}{1+A_i^n}),\\
\dot{C}_i &= \beta_3(-C_i + \frac{\alpha}{1+B_i^n} + \frac{\kappa S_i}{1+S_i}),\\
\dot{S}_i &= -k_{S0}S_i + k_{S1}B_i - \eta(S_i - S_{ext}),
\end{aligned} \qquad (1)$$

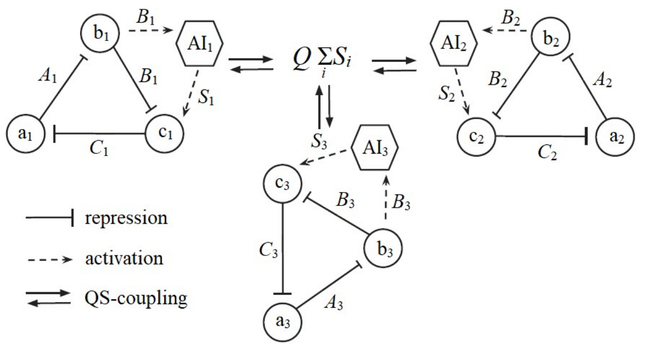

Fig. 1. Principle scheme of three coupled repressilator with quorum-sensing feedback.

where i = 1,2,3 for the three Repressilators, β_j (j = 1,2,3) are the ratios of the protein decay rate to mRNA decay rate, α accounts for the maximum transcription rate in the absence of an inhibitor, and n is the Hill cooperativity coefficient for inhibition. For the quorum sensing pathway k_{s0} is the ratio of the S decay rate to the mRNA decay rate, and as previously mentioned, k_{s1} is the rate of production of S and κ gives the strength of S activation of protein C. The diffusion coefficient η depends on the membrane permeability to the S molecule. The concentration of S in the external medium S_{ext} is determined according to quasi-steady state approximation by S produced by all Repressilators (S_1, S_2 and S_3) and a dilution factor Q:

$$S_{ext} = Q\frac{S_1 + S_2 + S_3}{3}. \qquad (2)$$

The model parameters are fixed in accordance with what was proposed in [10]: $\beta_1 = 0.5$, $\beta_2 = \beta_3 = 0.1$, $n = 3$, $k_{S0} = 1$, $k_{S1} = 0.01$, $\eta = 2$, $\kappa = 15$, α=2777. As control parameter, we use the coupling strength Q. In [9], it was shown that the occurrence of 2-dimensional and 3-dimensional torus is possible in model (1).

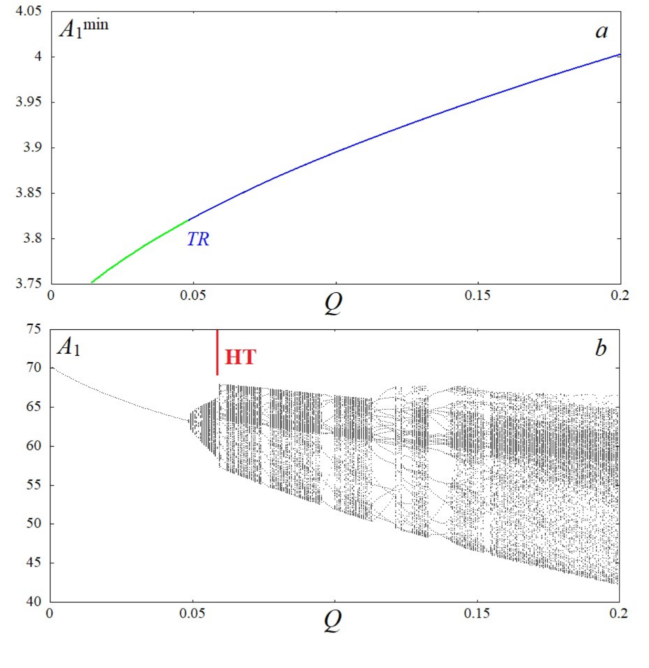

Fig. 2. Bifurcation diagram (a) and bifurcation tree for three ring oscillators (1). $\beta_1 = 0.5$, $\beta_2 = \beta_3 = 0.1$, $n = 3$, $k_{S0} = 1$, $k_{S1} = 0.01$, $\eta = 2$, $\kappa = 15$, α=2777. *TR* is point of Neimark-Sacker bifurcation. Green/Blue lines are stable/unstable cycles. **HT** is hard transition.

In Fig.2 bifurcation diagram obtained with XPPAUT [11] software package and bifurcation tree are presented. The base dynamical regime for ring oscillator (1) is rotating wave (RW) [9]: as a result of the identity of the oscillators, they have the same amplitudes, but each of the time realization is shifted by one third of the period relative to the next. With increasing of coupling strength RW undergoes the Neimark-Sacker bifurcation at Q≈0.04819 (*TR* in Fig.2a). This bifurcation is supercritical as a result two-frequency torus is softly born. Further increasing of coupling strength leads to hard transition (**HT** in Fig.2b) to another torus. Such hard transition can signify bistability. Further resonant cycles and development of chaos is observed (Fig. 2b).

III. Main Results

A. Bistable tori

Now let us consider in detail interval of coupling strength Q (0.045 - 0.062), where we observe bistability between two different tori. For tracking different tori we have found initial conditions for each of them at Q=0.0535, initial conditions is mentioned in caption to Fig.3. Then starting from them we scan interval parameter in two directions, and construct bifurcation trees presented in Fig.3a

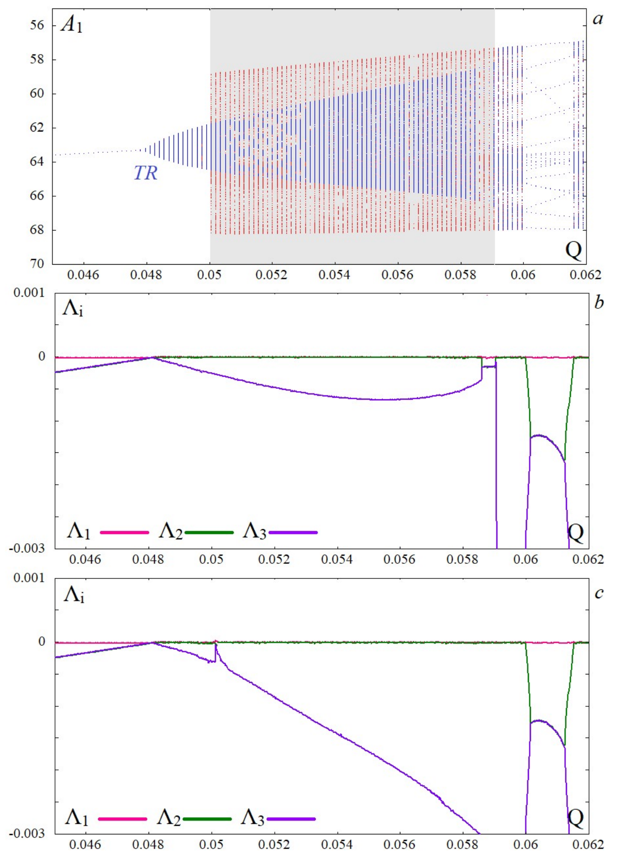

Fig. 3. Bifurcation trees (a) and spectrums of Lyapunov exponents (b, c) for three ring oscillators (1), demonstarting bi-stable tori. $\beta_1 = 0.5$, $\beta_2 = \beta_3 = 0.1$, $n = 3$, $k_{S0} = 1$, $k_{S1} = 0.01$, $\eta = 2$, $\kappa = 15$, α=2777. Initial conditions for Q=0.0535, 1) A_{10}=62.6, B_{10}=5.7, C_{10}=5.0, S_{10}=0.03, A_{20}=3.6, B_{20}=226.5, C_{20}=8.8, S_{20}=0.8, A_{30}=36.4, B_{30}=33.6, C_{30}=3.9, S_{30}=0.1; 2) A_{10}=58.6, B_{10}=5.8, C_{10}=5.0, S_{10}=0.04, A_{20}=2.7, B_{20}=339.6, C_{20}=9.8, S_{20}==1.2, A_{30}==4.2, B_{30}==195.8, C_{30}==8.3, S_{30}==0.7.

In interval Q [0.0502 - 0.0591] (grey color in Fig.3a) two different tori coexist. In Figs. 3b and 3c plots of the three largest Lyapunov exponents are presented, which were calculated for starting point Q=0.0535 with different initial conditions. Two-frequency oscillations are characterized by two zero Lyapunov exponents in the spectrum. In both plots of Lyapunov exponents it is clearly that first two exponents are zero. But third Lyapunov exponents are different. For the supercritical Neimark-Sacker bifurcation we can see typical dependence of the Lyapunov exponents near bifurcation point: for the values of parameter less then critical the largest Lyapunov exponent equals zero, and the second and the third are negative and equal each other. After bifurcation the second Lyapunov exponent becomes zero. At Q≈0.0502 in Fig.3c hard switching to the regime of another torus is observed. Such transition is typical for saddle-node bifurcation.

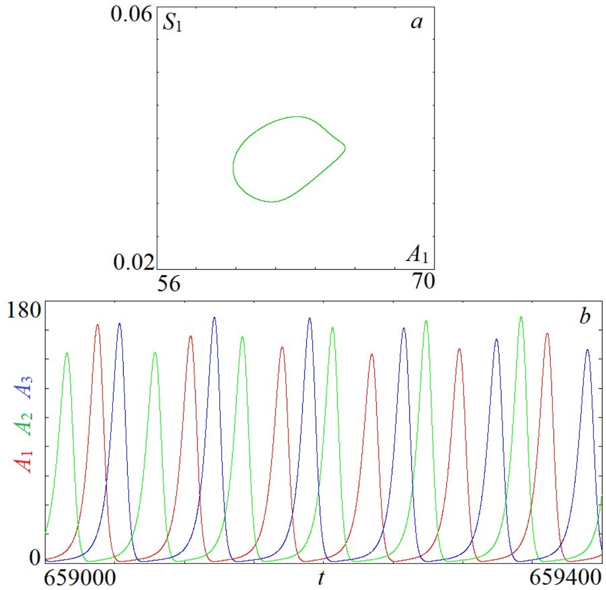

Fig. 4. Phase portrait in Poincarè section (a) and time series (b) for three ring oscillators (1) demonstarting torus occuring from RW-solution via Neimark-Sacker bifurcation.). $\beta_1 = 0.5$, $\beta_2 = \beta_3 = 0.1$, $n = 3$, $k_{S0} = 1$, $k_{S1} = 0.01$, $\eta = 2$, $\kappa = 15$, α=2777, Q=0.055.

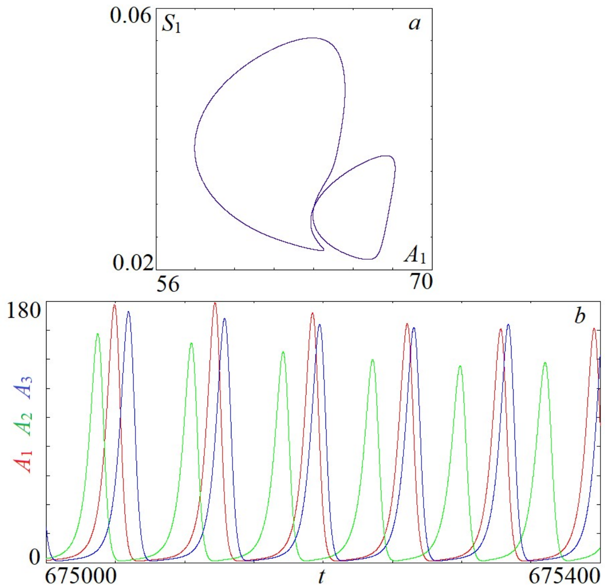

Fig. 5. Phase portrait in Poincarè section (a) and time series (b) for three ring oscillators (1) demonstarting torus occuring via saddle-node difurcation. $\beta_1 = 0.5$, $\beta_2 = \beta_3 = 0.1$, $n = 3$, $k_{S0} = 1$, $k_{S1} = 0.01$, $\eta = 2$, $\kappa = 15$, α=2777, Q=0.055

Let us consider a features of coexisting attractors. In Fig.4 phase portrait in Poincarè section by hypersurface C_1=5 and time series of the torus which is born as a result of supercritical Neimark-Sacker bifurcation are presented. The phase portrait in Poincarè section looks like smooth continuous invariant curve. Time series are shifted by one third of the period relative to the next.

In Fig. 5 phase portrait in Poincarè section by hypersurface C_1=5 and time series of the torus which is born as a result of saddle-node bifurcation are presented. The phase portrait in Poincarè section has more complex form, invariant curve has additional loop, but it still smooth and continuous. Time series are not shifted by one third of the period relative to the next, the phases differences between oscillators alternate being almost zero for two oscillators during some intervals of time.

B. Long transient dynamics

In recent paper [2] suggested that critical organization in a vicinity of a saddle-node bifurcation which is associated with formation so called saddle-node “ghost” enables transient memory of receptor. Formation of saddle-node "ghost" and such memory corresponds to the long transient dynamics near saddle-node bifurcation point. We would like to check the opportunity to observe saddle-node "ghost" in the case of occurrence torus bistability. We fix parameters near critical point, Q=0.0501, for this parameter there is only one torus, born via supercritical Neimark-Sacker bifurcation. But we take initial conditions for calculation near torus, corresponding to saddle-node bifurcation, the same as it used for Fig.3c, and examine attractors after different transient processes. In Fig.6a two phase portraits are shown. Black portrait corresponds to stable invariant curve, which we can reach after 1200 periods of transient oscillations. If we exclude the initial part of the transient time, for instance 100 periods, we can observe movement of the phase point on the surface of another torus, which is not born yet. If we change our parameter and fix it not so close to critical point, then it is enough 400 periods to reach invariant curve. In Fig.6b example of such phase portraits is presented. Thus, we observed long transient process corresponding to saddle-node "ghost" on the example of two-torus, which is disappear when we go far from critical point.

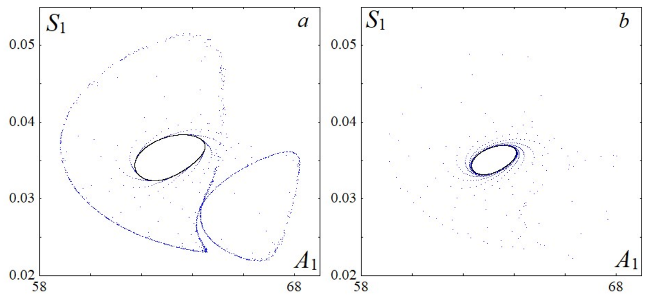

Fig. 6. Phase portraits in Poincarè section for three ring oscillators (1) demonstarting longtransient dynamics. $\beta_1 = 0.5$, $\beta_2 = \beta_3 = 0.1$, $n = 3$, $k_{S0} = 1$, $k_{S1} = 0.01$, $\eta = 2$, $\kappa = 15$, α=2777. *a*) Q=0.0501; b) Q=0.049. Black color is phase portrait without 1200 periods of transient process, blue color is phase portrait without 100 periods of transient process.

ACKNOWLEDGMENT

The work was carried out with the financial support of the Russian Foundation of Basic Research, grants No. 19-02-00610. Mechanism of torus bistability (Section III.A.) was described in the frame of grant Russian Science Foundation, No. 19-71-10048.

REFERENCES

[1] A.N. Pisarchik, U. Feudel, “Control of multistability,” Physics Reports, vol.540, No.4, 2014, pp. 167-218.

[2] A. Stanoev, A.P. Nandan, A. Koseska, “Organization at criticality enables processing of time-varying signals by receptor networks,” Molecular systems biology, vol.16, No.2, 2020, e8870.

[3] A. Koseska, et al, “Timing cellular decision making under noise via cell–cell communication,” PloS one, vol.4, No.3, 2009, e4872.

[4] N.V. Stankevich, E.I. Volkov, “Multistability in a three-dimensional oscillator: tori, resonant cycles and chaos”, Nonlinear Dyn. 2018. Vol. 94. No. 4. P. 2455-2467.

[5] M. Rosenblum, A. Pikovsky, “Self-organized quasiperiodicity in oscillator ensembles with global nonlinear coupling,” Phys. Rev. Lett., vol. 98, No.6, 2007, pp. 064101.

[6] A. Pikovsky, M. Rosenblum, “Self-organized partially synchronous dynamics in populations of nonlinearly coupled oscillators,” Physica D: Nonlinear Phenomena, vol. 238, No.1, 2009, pp. 27-37.

[7] M. Rosenblum, A. Pikovsky, “Two types of quasiperiodic partial synchrony in oscillator ensembles,” Phys. Rev. E, vol.92, No.1, 2015, pp. 012919.

[8] J. Garcia-Ojalvo, M.B. Elowitz, S. Strogatz, “Modeling a synthetic multicellular clock: repressilators coupled by quorum sensing,” Proceedings of the National Academy of Sciences, vol.101, No.30, 2004, pp. 10955-10960.

[9] N. Stankevich, E. Volkov, “Evolution of quasiperiodicity in quorum-sensing coupled identical repressilators,” Chaos: An Interdisciplinary Journal of Nonlinear Science, vol.30, No.4, 2020, pp. 043122.

[10] E.H. Hellen, E. Volkov, “Flexible dynamics of two quorum-sensing coupled repressilators,” Phys. Rev. E, vol.95, 2017, pp.022408.

[11] B. Ermentrout, Simulating, analyzing, and animating dynamical systems: a guide to XPPAUT for researchers and students, SIAM, 2002.